

EMSpice 2.0: Multiphysics Electromigration Analysis Tool for Beyond Moore ICs

Subed Lamichhane¹, Mohammadmir Kavousi¹ and Sheldon X.-D. Tan¹

¹Department of Electrical and Computer Engineering, University of California, Riverside, CA 92521
slami002@ucr.edu, mkavo003@ucr.edu, stan@ece.ucr.edu

Abstract—Electromigration (EM) remains a significant reliability challenge in current and future VLSI circuits. EM damage is projected to worsen due to increasing current density, even beyond Moore’s Law, as long as copper or metal interconnects are utilized. EMSpice was recently proposed to address fast EM sign-off analysis challenges, capable of performing full-chip EM-aware IR drop analysis for on-chip power grid networks. In this work, we introduce EMSpice 2.0, which incorporates interconnect Joule heating for the first time, considering the resulting thermal-induced atom migration (referred to as thermomigration, TM). EMSpice 2.0 accounts for Joule heating effects in EM stress evolution calculations and considers TM impacts on immortality checking, filtering mortal wires and expediting the analysis process. It considers three major atom migration forces: electrical, thermal, and stress-induced migrations, for more accurate EM lifetime analysis. Finite difference analysis is performed for both stress and temperature. Additionally, we have developed a user-friendly interactive interface and web portal (to be released) in Python for easy integration with existing design flows. Our results demonstrate that EMSpice 2.0 aligns well with industry standard finite element analysis tools such as COMSOL. Furthermore, EMSpice 2.0 offers a speedup of over 20× compared to state-of-the-art semi-analytical method and more than 220× speedup compared to COMSOL.

Index Terms—Electromigration, Full-Chip, Thermal-Aware

I. INTRODUCTION

Electromigration (EM) remains a significant reliability concern for current CMOS integrated circuit (IC) chips. It is anticipated that EM-induced damage or aging will exacerbate as technology advances, primarily due to increasing current density and smaller feature sizes. Even as technology progresses beyond Moore’s Law devices, EM-induced reliability issues may persist, particularly as long as copper or metal interconnects are utilized. Consequently, EM sign-off is critical in advanced technology nodes to ensure their long-term reliability [1]. EM is a physical phenomenon in which metal atoms migrate along the flow of electrical currents. As metal atoms leave the cathode of the wire, tensile stress develops, while simultaneously atoms accumulate at the anode, leading to compressive stress. This stress gradient formation counters the migration of atoms induced by the current, a phenomenon known as stress-migration, until an equilibrium is reached between the two forces. If the tensile stress exceeds a critical threshold, voids are nucleated and grow, resulting in increased wire resistance and potentially leading to open circuits. In addition to current-induced migration, temperature gradients, which can arise from Joule heating or active devices, can also cause atoms to move from regions of high temperature to low temperature, a phenomenon known as *thermomigration* (TM). The prevailing electromagnetic (EM) models utilized in industry, such as those by Black [2] and Blech [3], have faced criticism for their overly conservative nature and limited applicability to individual wire scenarios. Korhonen et al. [4] introduced a physics-based system of partial differential equations (PDEs) capable of assessing stress within each segment of interconnect wires. Various analytical and numerical methodologies have been proposed to tackle Korhonen’s equations for electromigration (EM) induced failure assessments. Cook et al. [5] introduced a numerical technique, termed *FastEM*, grounded in the finite difference method (FDM). This approach discretizes the PDEs into linear time-invariant ordinary differential equations (ODEs) before employing Krylov subspace-based reduction techniques to expedite computation.

This work is supported in part by NSF grant under No.CCF-2007135 and in part by NSF grant CCF-2305437.

Additionally, Chen et al. [6] presented an analytical solution for the PDEs to track stress evolution in interconnect structures.

However, most of the proposed analytical and numerical solutions overlook spatial temperature gradients resulting from Joule heating. Recent investigations [7] indicate that thermomigration (TM) induced by Joule heating can be nearly as significant as electromigration. With advancing technology leading to higher power densities and increased Joule heating, coupled with larger thermal resistances, these phenomena are exacerbated [8]. To mitigate these challenges, Kavousi et al. [9] proposed an EM stress analysis methodology explicitly considering the influence of thermomigration. Their work encompasses a method for estimating void saturation amidst spatial temperature gradients induced by Joule heating, addressing both nucleation and post-voiding phases. Furthermore, they leverage FDM extended by Krylov subspace methods to devise a rapid numerical solution for EM stress analysis, accounting for the effects of TM as well.

Although numerous numerical and analytical solutions have been proposed for electromigration (EM) stress analysis, these methods primarily focus on solving Korhonen’s equation itself. There has been little consideration of the time-dependent interaction between stress, void growth, wire resistance, and current densities. In addressing this gap, *EMSpice* [10] was introduced as a tool that integrates with commercial Electronic Design Automation (EDA) flows and provides comparisons on more practical Very Large Scale Integration (VLSI) layouts. *EMSpice* utilizes the finite difference method (FDM) for stress analysis in both nucleation and post-void phases. It offers visualization of both IR drop and stress distributions in power grid networks and can be integrated with existing commercial EDA flows.

Recently, another open-source EM analysis tool, *PROTON*, was proposed [11], also employing FDM for stress analysis. However, *PROTON* utilizes a commercial standard simulator for IR drop analysis, thereby lacking the close interplay between IR and EM effects provided by *EMSpice*. Furthermore, *PROTON* lacks an immortality check to filter out all EM immortal wires. While these proposed EM analysis tools can offer more accurate EM and IR drop analyses than existing models like Black’s, they still fail to consider Joule heating effects and resulting thermomigration (TM) effects for both immortality checks and stress analysis.

In this article, we present a full-chip TM-aware EM failure analysis tool, *EMSpice 2.0*, for physics-based coupled EM-TM and electronic analysis. Our tool takes power grid netlists from Synopsys ICC flow, and outputs the failed EM wires and their resistance changes and resulting IR drops of the power grids over the given aging time considering the joule heating effects. Our contribution is summarized as follows: (1) We present a user interactive full-chip electromigration analysis considering spatial joule heating and thermomigration(TM). This tool, called *EMSpice* encapsulates industry standard tool such as Synopsys ICC which provides a full design-to-failure analysis flow for a design. (2) We solve for current distribution due to joule heating and thermal convection more realistically starting from the basic principle of thermodynamics. This avoids unrealistic boundary condition assumptions, i.e both node of wires to be in same temperature. (3) The proposed method uses temperature aware EM immortality check for the trees in power grids of a given design for both nucleation and postvoiding phase. Immortality filtering filters out immortal wires and only mortal wires are solved for stress using Finite Difference Time Domain (FDTD) solver. This accelerates the

simulation process by more than 3 times. (4) Our FDTD based solver considers multiphysics interplay between EM stress, TM stress, IR drop, void growth, resistance change and current redistribution in a single framework. These consideration makes the EM analysis method more practical and accurate. (5) The backend of the tool contains fully python based immortality checker, fast and accurate FDM based stress solver and linear network IR drop solver. All the modules including the user interface modules are built using python. This makes the tool fast, easy to setup and easy to migrate between various platforms. (6) The proposed tool provides highly interactive user interfaces that enables easy input files selection, simulation execution and results visualization. The tool can be run by interactive Graphical User Interface(GUI), Command Line Interface(CLI) or can be used using a web based online portal without setting up the tool on their local machine. (7) Experimental results show that our TM aware FDTD based method is more than 20 times faster compared to state of the art semi-analytical TM aware method [7] and more than 220 times faster than conventional finite element method(FEM) based COMCOL [12] without significant loss in the accuracy.

This paper is organized as follows: The details on implementation of our tool is presented in Section II. Section III reviews the physics behind temperature aware immortality check and stress evolution. Section IV presents experimental results on our case study. Finally, Section V summarizes the conclusions on this work.

II. THE ARCHITECTURE OF EMSPICE 2.0

In this section, we present the architecture and flow of the proposed EMspice 2.0 tool. EMspice 2.0 consists of a simulation engine, a user interface, and a data interface for integration into commercial Electronic Design Automation (EDA) flows. The tool is designed to be highly interactive, facilitating the input of design parameters, electrical specifications, and electromagnetic (EM) characteristics, while providing output results through interactive visual aids. As illustrated in Fig. 1, our framework incorporates the Synopsys ICC (IC Compiler II) design flow for reading the design files. Synopsys ICC is a leading tool in physical synthesis within the industry, capable of generating crucial physical geometry, current, voltage, and power information for the power delivery network (power grids) of the design. This information is then formatted into a SPICE (.sp) file. When EMspice 2.0 reads the SPICE file and parameter file containing all the necessary parameters for electromagnetic (EM) simulation, the tool parses the SPICE file to extract position, length, width, resistance, current, and voltage information for the power grids. This information is utilized to perform an immortality filter, which excludes immortal wires from stress analysis, thus saving significant computational costs. Specifically, the tool first applies the nucleation phase filtering condition (shown in the following section as Eq. 9) to the trees. Trees that are determined to be immortal during the nucleation phase are filtered out, leaving only mortal wires for further analysis. These mortal wires then undergo a post-voiding phase immortality check (as described in Eq. 13). In the post-voiding phase, trees where void volumes cannot exceed a critical volume are filtered out as immortal. Only the trees for which the resistance could change are further analyzed. The linear network IR drop solver employs modified nodal analysis (MNA) to solve for time-dependent current density, while the fast electromigration-therm migration (EM-TM) solver utilizes this current density information to calculate the resulting stress for all mortal trees. As voids form, the resistances on the trees change. For each time step, the EM-TM solver updates resistance information and provides it to the IR drop solver. Subsequently, the IR drop solver solves for the updated current density information and feeds it back to the EM-TM solver to calculate the resulting stress distribution. This tool is fully implemented in Python only, which makes this tool easy to set up and platform-independent. The tool can be used either via command line interface (CLI) as depicted in Fig. 2a, or through a graphic user interface (GUI) as shown in Fig. 2b. The command line version initializes an environment supporting commands to run simulations. Simulations are executed using commands with arguments that specify input files and parameter files. The GUI

mode offers a more interactive experience. Implemented using the Python tkinter library, a standard Python library known for its simplicity and cross-platform compatibility, the GUI avoids dependency-related issues common with external libraries like PyQt.

Upon receiving power grid information, the tool invokes an interactive visualization window, as depicted in Fig. 2c. This window offers a flexible interface for visualizing the geometry of the power grids and current distribution. Users can provide input to select trees and tree branches for visualization. Upon completion of the simulation, another interactive window, as shown in Fig. 2d, appears. This window allows users to select wires at the branch level to plot the calculated stress distribution. Users can visualize the stress distribution, save the plot, and import the stress distribution to a file. We have further implemented a web application version of our tool, referred to as the *online portal* (to be released to public soon). As illustrated in Fig. 3, the online portal enables users to upload an input power grid information file in SPICE format, as well as the required parameter files for simulation. Once the user provides these files, the simulation is conducted on the server hosting the online portal. The results, including the power grid structure, current distribution, temperature distribution, and stress distribution, are then displayed on the online portal page, where users can download them.

III. KEY COMPUTING STEPS OF EMSPICE 2.0

In this section, we provide a brief overview of the physics model of electromigration (EM) stress evolution and outline the key computational steps in EMspice 2.0. Failure due to electromigration is a gradual and cumulative process resulting from the interaction between metal atoms in the power grid and conducting electrons. This interaction causes the migration of metal atoms, leading to tensile stress at cathode nodes and compressive stress at anode nodes of the metal wires. These stresses can create voids at cathode ends and hillocks at anode nodes, which can ultimately lead to failure (increased resistance or open circuits) of the metal wires. The period during which voids nucleate is referred to as the nucleation phase, while the period after nucleation is typically known as the post-voiding phase. In summary, three main physical forces drive the atomic flux and alter the concentration of metal atoms: electromigration (EM), stress migration (SM), and thermomigration (TM) [13], [14].

The EM stress σ considering EM, SM and TM can be solved using following form of Korhonen's equation [15]:

$$\frac{\partial \sigma}{\partial t} = \frac{\partial}{\partial x} \left[k(x) \left(\frac{\partial \sigma}{\partial x} - \frac{eZ\rho j}{\Omega} - \frac{Q}{\Omega T} \frac{\partial T}{\partial x} \right) \right] \quad (1)$$

here, $k(x) = D_a(T(x))B\Omega/(k_B T(x))$ is diffusivity, with $D_a = D_0 \exp(-E_a/k_B T)$ is atomic diffusion coefficient, D_0 is a constant, E_a is the EM activation energy.

The transient hydro-static stress evolution ($\sigma(x, t)$) for a general interconnect structure at nucleation phase is described by the Korhonen equation as:

$$\text{PDE: } \frac{\partial \sigma}{\partial t} = \frac{\partial}{\partial x} \left[\kappa(x) \left(\frac{\partial \sigma}{\partial x} - S - M \right) \right], \quad t > 0 \quad (2)$$

$$\text{BC: } \kappa(x_b) \left(\frac{\partial \sigma}{\partial x} \Big|_{x=x_b} - S - M \right) = 0, \quad 0 < t < t_{\text{nuc}} \quad (3)$$

$$\text{IC: } \sigma(x, 0) = \sigma_T \quad (4)$$

Here, $S = \frac{eZ\rho j}{\Omega}$ is EM flux, $M = \frac{Q}{\Omega T} \frac{\partial T}{\partial x}$ is for TM flux, $\kappa(x) = D_a(T(x))B\Omega/(k_B T(x))$ is position dependent diffusivity due to non-uniform temperature, where $D_a = D_0 \exp(-E_a/k_B T)$ is atomic diffusion, D_0 is a constant, E_a is the EM activation energy, σ_T is the initial thermal induced residual stress and x_b represents the block terminals.

A. Temperature distribution in interconnect structure

Eq 2 is solved with the aid of boundary conditions 3 and initial conditions to determine the stress distribution on the trees within the power grid. However, to calculate the temperature effects on immortality checks and EM stress solutions, the first requirement is the temperature distribution on the trees within the power grid. Existing models used to calculate temperature

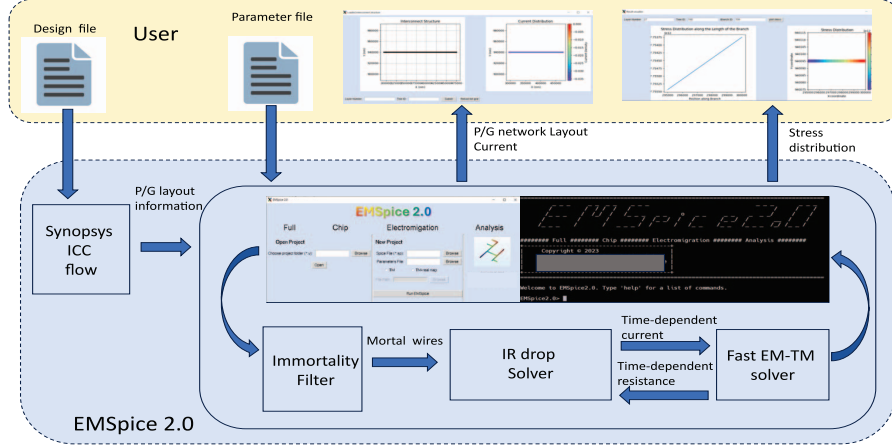


Fig. 1: Overall framework of the proposed EMSpice 2.0

distribution are not suitable for long wires, as they mostly focus on temperature distribution for end-to-end single wires and assume both ends to be at the same temperature [13]. Beginning from the first law of thermodynamics, the thermal behavior of a solid region over time is described by [16]:

$$\rho_m c_p \frac{\partial T}{\partial t} + \nabla q = Q \quad (5)$$

where, c_p is specific heat capacity, ρ_m is the mass density, $q = -k\nabla T$ is the component due to heat flux described by Fourier's law, $Q = Q_{jh} + Q_{conn}$ is the component due to Joule heating and heat convection. Here, $Q_{jh} = j^2 \rho$ and $Q_{conn} = k(T - T_0)/\Gamma^2$. Γ is the thermal characteristic length that depends on the geometry and topology of the surroundings and can be approximated as follows [13]:

$$\Gamma^2 = t_{cut} ILLD \frac{k_{cu}}{k_{CLD}} \quad (6)$$

here, t_{cu} and k_{cu} are thickness and thermal conductivity of the wire, and t_{ILD} and k_{ILD} are thickness and conductivity of dielectric.

For stationary condition, Eq 5 becomes:

$$k\nabla^2 T - (j^2 \rho + k(T_0 - T)/\Gamma^2) = 0 \quad (7)$$

Eq 7 can be solved numerically using FDM, FEM based methods to get spatial temperature distribution. The temperature solution for single wire with boundary conditions $T(-L/2) = T_1$ and $T(+L/2) = T_2$ can also be approximated by [13], [14]:

$$T(x) = T_0 + T_m \left[1 - \frac{\cos\left(\frac{x}{\Gamma}\right)}{\cos\left(\frac{L}{2\Gamma}\right)} \right] + T_n \left[1 - \frac{\sin\left(\frac{x}{\Gamma}\right)}{\sin\left(\frac{L}{2\Gamma}\right)} \right] \quad (8)$$

B. Temperature-aware mortality check for nucleation and post-voiding phase

During the nucleation phase of the EM stress evolution, the stress at the cathode node increases over time. In this phase, if the stress on the cathode node at steady state (σ_{steady}) is lower than the critical stress ($\sigma_{critical}$), then the tree is considered to be immortal during the nucleation phase. We can use a voltage-based immortality check to assess the immortality of the trees during both the nucleation phase, considering the temperature effect, as described by Sun and Demircan [17] and Sun and Cook [18]:

$$\nu_{crit,EM}^T > \nu_E^T - \nu_{cat}^T \quad (9)$$

here ν_{cat}^T is the voltage at the cathode. $\nu_{crit,EM}$ is critical EM voltage defined by

$$\nu_{crit,EM}^T = \frac{1}{\beta} (\sigma_{crit} - \sigma_{init}) \quad (10)$$

Where σ_{init} is the initial stress and σ_{crit} is the critical stress. In Eq 9, ν_E is the EM voltage given by

$$\nu_E^T = \frac{1}{2A} \sum_{i \neq c} a_i \nu_i^T \quad (11)$$

Here ν_i is the normal nodal voltage (with respect to cathode node c) at node i , a_i is the total area of branches connected to node i , a_i and A is the total area of the wire.

At post-voiding phase, voids are formed on trees that do not pass the immortality check at nucleation phase. The void will keep growing until it is saturated. If the saturation volume of the void is smaller than critical volume, the wire is still immortal [10]. For immortality check in this phase, the saturated volume is compared with the critical volume as described by this equation.

$$V_{crit} > V_{sat} \quad (12)$$

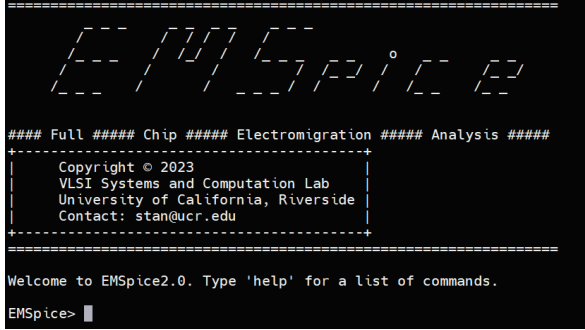
If we consider the spatial temperature distribution, we have to reconsider the calculation of the saturation volume [9]. Immortality condition considering the temperature effect can be described as:

$$V_{sat,k}^T < V_{sat,crit}^T \quad (13)$$

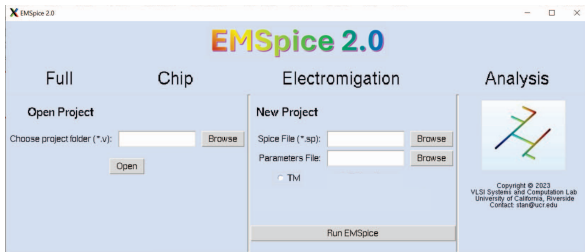
Here, $V_{sat,crit}^T$ is the given critical volume before any resistance changes can happen in a wire. $V_{sat,k}^T$ is the saturation volume for k th void for a tree with N_k branches, which is estimated by:

$$\begin{aligned} V_{sat,k}^T = & -\frac{1}{B} \sum_{ij} w_{ij} h_{ij} \left[\left(\frac{\sigma_i + \sigma_j}{2} \right) L_{ij} \right. \\ & + \frac{Q}{\Omega} \left(\ln \left(\frac{T_0 + T_{m,ij}}{\sqrt{T_i T_j}} \right) L_{ij} \right. \\ & \left. \left. + \frac{(T_i + T_j - 2(T_0 + T_{m,ij}))\Gamma}{T_0 + T_{m,ij}} \tanh \left(\frac{L_{ij}}{2\Gamma} \right) \right) \right] \\ & + \sum_{ij} \frac{w_{ij} h_{ij} L_{ij}}{B} \frac{eZ}{\Omega} (\nu_E^T - U_g^T) \\ & + \sum_{ij} \int_{x_i}^{x_j} w_{ij} h_{ij} \frac{\sigma_0}{B} dx \end{aligned} \quad (14)$$

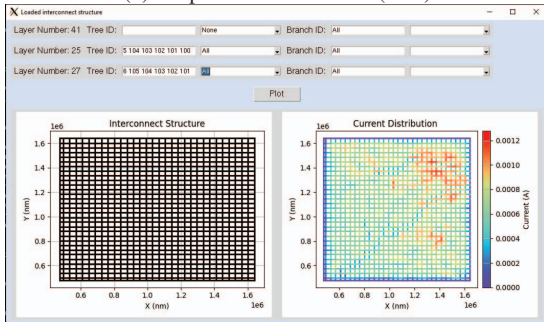
here, B is the effective bulk elasticity modulus, e is the electron charge, Z is the effective charge number, Ω is the atomic lattice volume, Q is the specific heat of transport, w_{ij} , h_{ij} and L_{ij} are the width, height and length of the branch ij , ν_E^T is EM voltage considering spatial effect, $U_g^T =$



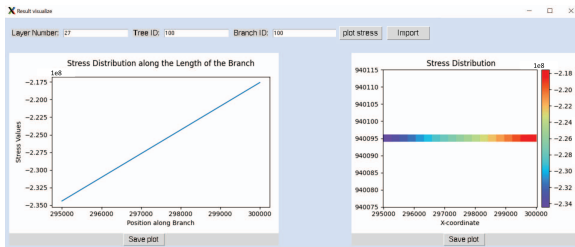
(a) Command line interface (CLI)



(b) Graphical user interface (GUI)



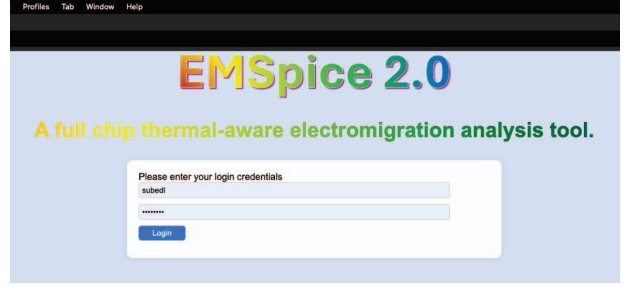
(c) Example of a power grid structure and current distribution visualization



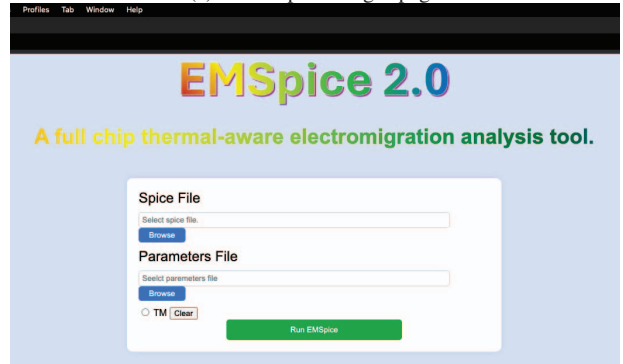
(d) Stress distribution results visualization

Fig. 2: EMSpice 2.0 user interface (command line or graphic), visualization of the results.

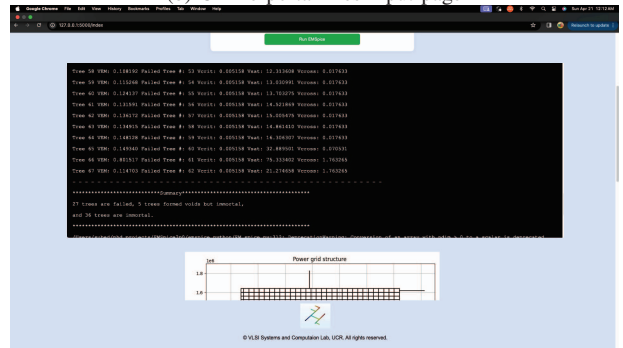
$U_g - \frac{Q}{eZ} \ln(T_g)$ where U_g and T_g are the temperature and voltage at node g with maximum stress. T_0 is the ambient temperature, $T_m = \frac{j^2 \rho \Gamma^2}{\kappa C_u}$, $T_n = \frac{T_i - T_j}{2}$ where ρ is resistivity and κC_u is the thermal conductivity.



(a) Online portal login page



(b) Online portal files input page



(c) Online portal simulation progress and result visualization

Fig. 3: Illustration of online portal pages.

C. EM stress calculation considering TM using FDM

Korhonen's equation considering EM, SM and TM, Eq 2 is solved along with the BCs and IC using FDTD for each multi-segment interconnect tree for stress analysis over time. As we perform the finite difference, the differential equation Eq 2 along with BCs and IC is converted to the linear time invariant (LTI) system represented by:

$$C\dot{\sigma}(t) = A\sigma(t) + B_j(t) - D \quad (15)$$

Here, $\sigma(t)$ represents the stress vector, C , A are $n \times n$ matrices, D is $n \times 1$ constant matrix corresponding to TM effect, B is $n \times p$ input matrix, p being the input size. Krylov subspace based method is used to solve this ODE LTI stress evolution system. Here, $\sigma(0)$ is the initial stress, whose value is residual stress at time = 0 and stress from previous simulation step for each new simulation step. Finally, the coupled EM-TM-IR drop partial derivative equations we solve in this paper can be

expressed as:

$$\begin{aligned}
 C\dot{\sigma}(t) &= A\sigma(t) + B_j(t) - D \\
 V_v(t) &= \int_{\Omega_L} \frac{\sigma(t)}{B} dV \\
 G(t) \times u(t) &= P_j(t) \\
 \sigma(0) &= [\sigma_1(0), \sigma_2(0), \dots, \sigma_n(0)]
 \end{aligned} \tag{16}$$

Where, $V_v(t)$ is expression to estimate the void volume in a wire, Ω_L is the volume of the remaining of the wire, V is the volume of the wire. For IR drop, simple resistance network is extracted from the power grid network and Modified Nodal Analysis(MNA) is applied as shown in 16. $G(t)$ here represents the admittance matrix for the power grid network which is time varying as resistance changes due to EM-TM effect.

For post-voiding phase, PDE is the same as nucleation phase and IC is the stress at $t = t_{nuc}$, in the nucleation phase, the BC at the position where the void is nucleated is represented as:

$$\left. \frac{\partial \sigma}{\partial x} \right|_{x=x_{nuc}} = \frac{\sigma(x_{nuc}, t)}{\delta}, \quad t_{nuc} < t < \infty \tag{17}$$

Here, x_{nuc} is the position of the void nucleation at the boundary and δ is the thickness of the void surface. A LTI ODE system similar to 16 can be obtained with this BC for post-voiding phase as well and can be solved accordingly.

As the void continues to grow in the post-voiding phase, the wire resistances start to change after the void volume exceed the critical volume V_{crit} . This changes the current density since now the current has to flow over the highly resistive $T_a/T_a N$ barrier whose resistance is higher than wire resistance. The wire resistance change can be approximated as [10]:

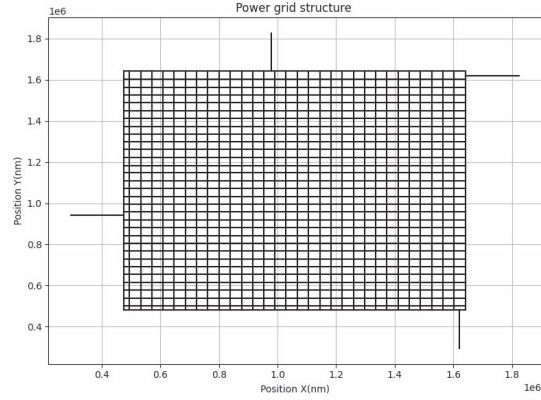
$$\Delta R(t) = \frac{V_v - V_{crit}}{WH} \left[\frac{\rho T_a}{h_{T_a}(2H + W)} - \frac{\rho C_u}{HW} \right] \tag{18}$$

For each time step of FDTD EM-TM simulations, $\Delta R(t)$ is calculated and the current distribution is recalculated for next simulation step to account for the resistance change due to void volume growth.

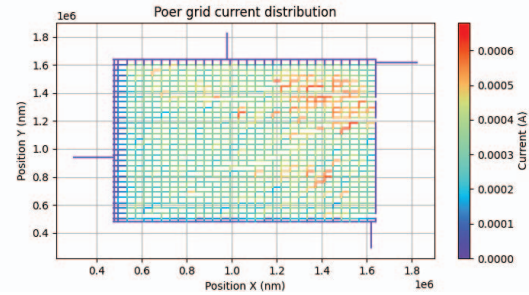
IV. NUMERICAL RESULTS AND DISCUSSIONS

In this section, we present numerical comparison results of the proposed EMspice 2.0, which is fully implemented in Python 3. The modules, including the IR drop solver, FDTD EM-TM analysis, command line interface (CLI), graphical user interface (GUI), and online portal, are all implemented in Python. The case studies were conducted on a Linux server equipped with Intel 22-core E5-2699 CPUs and 320GB of memory.

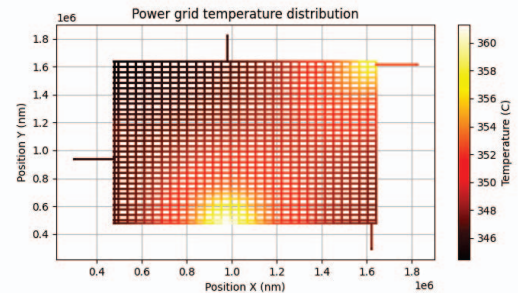
Using the proposed method, full-chip electromigration analysis can be performed with high accuracy and efficiency. Beginning with an RTL design, we utilize Synopsys IC design tools to extract geometrical and electrical information of the power grid. Subsequently, simulations are conducted. Additionally, our tool offers highly interactive interfaces including CLI, GUI, and an online portal for input, simulation execution, and visualization of results. To illustrate, we consider the *Cortex-M0 (ARMv6-M)* design as an example. We use Synopsys IC design tools with the Synopsys 32/28nm library to synthesize and simulate the design, obtaining geometry and electrical information. Fig. 4a displays the power grid structure of the *Cortex-M0 (ARMv6-M)* design, which comprises 68 straight trees routed in two layers. Fig. 4b depicts the current distribution on the branches of the trees within the power grid, obtained through simulations in the Synopsys IC design tool. Fig. 5b shows the temperature distribution on the considered power grid. Fig. 4d illustrates the stress distribution on the mortal trees within the power grid under study. Notably, immortal wires, depicted as plain black lines, are filtered out. Utilizing temperature-aware immortality filtering, 41 trees are identified as immortal. Among these, 36 trees are identified as nucleation phase immortal, while 5 are post-voiding phase immortal. Only 39% of the trees are further processed for FDTD EM-TM stress calculation. This filtering reduces the total stress calculation time by almost threefold.



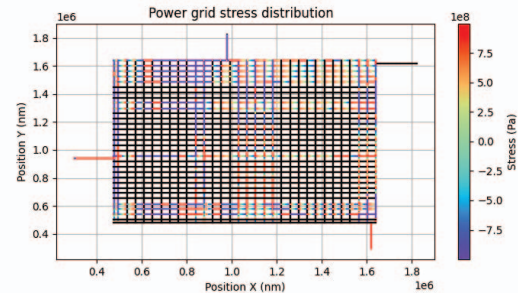
(a) One example of a on-chip power grid structure



(b) The example of current distribution in the power grid

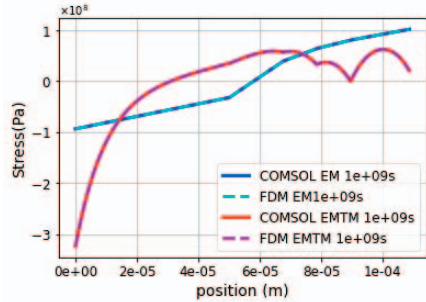


(c) The example of temperature distribution in a power grid

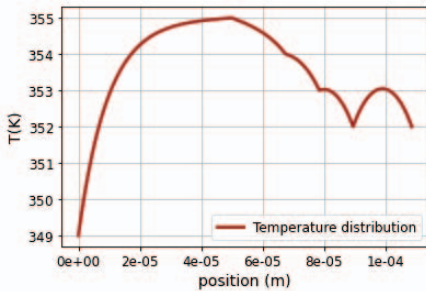


(d) The example of stress distribution on mortal trees of a power grid

Fig. 4: Visualization of geometry, current distribution, temperature distribution and stress distribution over the PDN of Cortex design



(a) Comparison of stress distribution result from proposed method against COMSOL using considering EM only and EM-TM at $t=1e10$ s



(b) Temperature distribution used in the above stress calculation

Fig. 5: Stress result comparison and temperature distribution used for the stress

For the EM-TM stress solver method, we randomly selected 20 trees from the *Cortex* power grid and solved them using COMSOL. The stress results obtained using the temperature-aware FDM method agree very well with those from COMSOL [12], as shown in Fig. 5. The interconnect tree depicted in the figure is a five-segment tree selected from a *Cortex* tree for better illustration. Fig. 5b shows the temperature distribution in the interconnect tree. The stress on the solved trees ranged from -7×10^8 Pa to 8.3×10^8 Pa. The average root mean square error (RMSE) for the stress obtained using our proposed method compared to COMSOL is found to be 3.7×10^7 , translating to an average error of around 1.88%.

Furthermore, to analyze performance, we solved another 20 randomly selected trees from the *Cortex* power grids using the proposed method, COMSOL, and the state-of-the-art semi-analytical method proposed in [7]. The average number of branches in the trees in this design is 33. For the 20 randomly selected trees, the average runtime for our tool is found to be 1.4 seconds. Using the semi-analytical approach, the average runtime is found to be 29.7 seconds. For COMSOL, the average runtime is observed to be around 315 seconds. From these observations, we can conclude that the proposed FDTD-based method is more than 20 times faster than the method in [7] and more than 220 times faster than the FEM-based tool COMSOL.

V. CONCLUSIONS

In this paper, we introduced a new generation of coupled electromigration (EM) aware IR drop analysis for on-chip power grid networks: EMspice 2.0. This tool provides, for the first time, fast and accurate temperature-aware mortality checks to accelerate the failure analysis process. Additionally, it features a highly user-friendly interface, fast mortality net filtering, and tight integration of the industry-standard Synopsys ICC physical synthesis for easy EM sign-off analysis. The backend of this tool utilizes FDTD-based fast and accurate coupled IR drop-EM-TM stress solvers. Implemented solely in the Python programming language, this tool is easy to set up and platform-independent. It offers a highly interactive user

experience through both a graphical user interface and a web-based online portal with flexible simulation and visualization support. Experimental results demonstrate that the proposed FDTD-based method can achieve more than a 20-fold speedup compared to state-of-the-art semi-analytical methods and more than a 220-fold speedup compared to the FEM-based tool COMSOL.

REFERENCES

- [1] S. X.-D. Tan, M. Tahoori, T. Kim, S. Wang, Z. Sun, and S. Kiamehr, *VLSI Systems Long-Term Reliability – Modeling, Simulation and Optimization*. Springer Publishing, 2019.
- [2] J. R. Black, "Electromigration-A Brief Survey and Some Recent Results," *IEEE Trans. on Electron Devices*, vol. 16, no. 4, pp. 338–347, Apr. 1969.
- [3] I. A. Blech, "Electromigration in thin aluminum films on titanium nitride," *Journal of Applied Physics*, vol. 47, no. 4, pp. 1203–1208, 1976.
- [4] M. A. Korhonen, P. Borgesen, K. N. Tu, and C. Y. Li, "Stress evolution due to electromigration in confined metal lines," *Journal of Applied Physics*, vol. 73, no. 8, pp. 3790–3799, 1993.
- [5] C. Cook, Z. Sun, E. Demircan, M. D. Shroff, and S. X.-D. Tan, "Fast electromigration stress evolution analysis for interconnect trees using krylov subspace method," *IEEE Trans. on Very Large Scale Integration (VLSI) Systems*, vol. 26, no. 5, pp. 969–980, May 2018.
- [6] H. Chen, S. X.-D. Tan, X. Huang, T. Kim, and V. Sukharev, "Analytical modeling and characterization of electromigration effects for multibranch interconnect trees," *IEEE Trans. on Computer-Aided Design of Integrated Circuits and Systems*, vol. 35, no. 11, pp. 1811–1824, 2016.
- [7] L. Chen, S. X.-D. Tan, Z. Sun, S. Peng, M. Tang, and J. Mao, "A fast semi-analytic approach for combined electromigration and thermomigration analysis for general multisegment interconnects," *IEEE Transactions on Computer-Aided Design of Integrated Circuits and Systems*, vol. 40, no. 2, pp. 350–363, 2021.
- [8] A. Todri, S. Kundu, P. Girard, A. Bosio, L. Dilillo, and A. Virazel, "A study of tapered 3-d TSVs for power and thermal integrity," *IEEE Transactions on Very Large Scale Integration (VLSI) Systems*, vol. 21, no. 2, pp. 306–319, Feb 2013.
- [9] M. Kavousi, L. Chen, and S. X.-D. Tan, "Fast electromigration stress analysis considering spatial joule heating effects," in *2022 27th Asia and South Pacific Design Automation Conference (ASP-DAC)*, 2022, pp. 208–213.
- [10] Z. Sun, S. Yu, H. Zhou, Y. Liu, and S. X.-D. Tan, "EMSpice: Physics-Based Electromigration Check Using Coupled Electronic and Stress Simulation," *IEEE Transactions on Device and Materials Reliability*, vol. 20, no. 2, pp. 376–389, Jun. 2020.
- [11] O. Axelou, E. Tselepi, G. Floros, N. Evmorfopoulos, and G. Stamoulis, "Proton – a python framework for physics-based electromigration assessment on contemporary vlsi power grids," in *2023 19th International Conference on Synthesis, Modeling, Analysis and Simulation Methods and Applications to Circuit Design (SMACD)*, 2023, pp. 1–4.
- [12] C. Multiphysics, "Heat transfer module user's guide," *COMSOL version*, vol. 4, 2014.
- [13] A. Abbasinasab and M. Marek-Sadowska, "RAIN: A tool for reliability assessment of interconnect networks—physics to software," in *Proc. Design Automation Conf. (DAC)*. New York, NY, USA: ACM, 2018, pp. 133:1–133:6.
- [14] M. Kavousi, L. Chen, and S. X.-D. Tan, "Electromigration Immortality Check considering Joule Heating Effect for Multisegment Wires," in *Proc. Int. Conf. on Computer Aided Design (ICCAD)*, 2020, pp. 1–8.
- [15] R. de Orto, H. Ceric, and S. Selberherr, "Physically based models of electromigration: From black's equation to modern tead models," *Microelectronics Reliability*, vol. 50, no. 6, pp. 775–789, 2010, 2009 Reliability of Compound Semiconductors (ROCS) Workshop. [Online]. Available: <https://www.sciencedirect.com/science/article/pii/S0026271410000193>
- [16] H. S. Carslaw and J. C. Jaeger, *Conduction of Heat in Solids*, 2nd ed. Oxford: Oxford University Press, 1959.
- [17] Z. Sun, E. Demircan, M. D. Shroff, T. Kim, X. Huang, and S. X.-D. Tan, "Voltage-Based Electromigration Immortality Check for General Multibranch Interconnects," in *Proc. Int. Conf. on Computer Aided Design (ICCAD)*, Nov. 2016, pp. 1–7.
- [18] Z. Sun, E. Demircan, M. D. Shroff, C. Cook, and S. X.-D. Tan, "Fast Electromigration Immortality Analysis for Multisegment Copper Interconnect Wires," *IEEE Trans. on Computer-Aided Design of Integrated Circuits and Systems*, vol. 37, no. 12, pp. 3137–3150, Dec. 2018.